H. Ostrom, *Science* **170**, 537 (1970)].
4. The Eichstätt specimen was elevated to a separate species (then genus) by correlation of qualitative tooth characters with inferred diet, proportional differences in limbs, absence of a furcula, and supposed differences in the orientation of the pubis (which is disarticulated in all specimens) [M. E. Howgate, *Zool. J. Linn. Soc.* **82**, 159 (1984); in *The Beginnings of Birds, Proceedings of the International* Archaeopteryx *Conference 1984*, M. K. Hecht, J. H. Ostrom, G. Viohl, P. Wellnhofer, Eds. (Freunde des Jura-Museums, Eichstätt, 1985), pp. 105–112].
5. P. Wellnhofer, *Science* **240**, 1790 (1988).
6. J. A. Gauthier, *Mem. Cal. Acad. Sci.* **8**, 1 (1986). *Archaeopteryx* is a metaspecies (no evidence for either monophyly or paraphyly) [M. J. Donoghue, *Bryologist* **88**, 172 (1985)].
7. For example, P. Dodson, *J. Zool.* **175**, 315 (1975).
8. G. Callison and H. M. Quimby, *J. Vertebr. Paleontol.* **3**, 200 (1984).
9. S. J. Gould, *Am. Nat.* **105**, 113 (1971).
10. S. S. Sweet, *Am. Zool.* **20**, 643 (1980); R. E. Strauss, *Syst. Zool.* **34**, 381 (1985).
11. *Theropods*: birds and all saurischian dinosaurs that are phylogenetically closer to birds than to sauropodomorphs; *coelurosaurs*: birds and all other theropods that are phylogenetically closer to birds than to Carnosauria (*6*).
12. P. Wellnhofer, *Palaeontogr. Abt. A Palaeozool. Stratigr.* **147**, 169 (1974); J. H. Ostrom, *Biol. J. Linn. Soc.* **8**, 91 (1976); see also (*6*). Retained subadult characteristics of coelurosaurs: free cervical ribs, separate sacral vertebrae, and an unfused scapulocoracoid. Most extant birds have a ball-and-socket joint between the scapula and coracoid which never fuses. The scapula and coracoid fuse when growth ceases in extant ratites which (like *Archaeopteryx*, *Hesperornis*, and other dinosaurs) do not have such a joint. The subadult status may also account for the lack of an ossified sternum [G. DeBeer, *Archaeopteryx lithographica*, British Museum (Natural History), London (1954)]. Sternal ossification appears late in the development of extant birds and other full-grown theropods, this condition pre-dates the origin of birds (*6*).
13. For example, *Leipoa ocellata* (mallee fowl) and *Alectura lathami* (brush turkey) [M. M. Nice, *Trans. Linn. Soc. N.Y.* **8**, 1 (1962); D. Vleck, C. Vleck, R. S. Seymour, *Physiol. Zool.* **57**, 444 (1984)].
14. R. E. Ricklefs, *Ibis* **115**, 191 (1973).
15. Conclusions are vulnerable to four limitations; "size" for extant species commonly being reported as mass (rarely as relative bone dimensions) and the small number of directly comparable data sets; the paucity of ontogenetic skeletal series for extant species; the fragmentary nature of the fossil record; and the inherent entanglement of ontogenetic and phylogenetic patterns.
16. D. Pilbeam and S. J. Gould, *Science* **186**, 892 (1974); P. Dodson, *Syst. Zool.* **24**, 37 (1975); F. E. Grine *et al.*, *S. Afr. J. Sci.* **74**, 50 (1978).
17. D. Carrier, *J. Zool. (London)* **201**, 27 (1983).
18. From: P. Wellnhofer, *Palaeontogr. Abt. A. Palaeozool. Stratigr.* **147**, 169 (1974). All dimensions where three or more specimens were measurable were included.
19. Multivariate allometric coefficients (α_m) are with respect to general size [F. L. Bookstein, *Syst. Zool.* **38**, 173 (1989)]. General size was estimated as the major axis, equivalent to the first eigenvector of the covariance matrix. Allometries (α_m) were estimated as growth rates of characters with respect to general size, scaled to a mean of one = isometry. All measurements were log-transformed to ensure homoscedasticity and to linearize allometric scaling effects [P. Jolicoeur, *Biometrics* **19**, 497 (1963)].
20. The conclusion of a single growth trajectory is parsimonious and consistent with the data. In the absence of diagnostic characters for *Archaeopteryx*, however, we cannot exclude heterochrony via hypermorphosis or progenesis (identical growth trajectories, differing only in adult size), which can occur in closely related taxa (for example, species flocks).
21. If *Archaeopteryx* contained more than one taxon, larger specimens might have had relatively larger distal femora. They do not (Eichstätt: $\alpha_m = 0.12$; Berlin: $\alpha_m = 0.10$; and London: $\alpha_m = 0.12$).
22. H. D. Prange, J. F. Anderson, H. Rahn, *Am. Nat.* **113**, 103 (1979).
23. J. H. Ostrom, *Am. Sci.* **67**, 46 (1979).
24. D. Carrier and L. R. Leon, *J. Zool. (London)*, in press.
25. J. A. Gauthier, unpublished observation.
26. R. E. H. Reid, *Symp. Zool. Soc. London* **52**, 629 (1984).
27. J. A. Gauthier, M. A. Houck, R. E. Strauss, in preparation.
28. We thank P. Wellnhofer for his encouragement and for sharing his manuscript on the new Solnhofen specimen. We thank D. Carrier for his unpublished manuscript. B. Calder, D. Carrier, C. Vleck, and D. Vleck critically edited the manuscript. Supported by NSF grants BSR 83-07711 to M.A.H., BSR-87-09455 to J.A.G., and BSR 83-07719 to R.E.S.

12 July 1989; accepted 31 October 1989

Global Climate Change and Intensification of Coastal Ocean Upwelling

ANDREW BAKUN

A mechanism exists whereby global greenhouse warming could, by intensifying the alongshore wind stress on the ocean surface, lead to acceleration of coastal upwelling. Evidence from several different regions suggests that the major coastal upwelling systems of the world have been growing in upwelling intensity as greenhouse gases have accumulated in the earth's atmosphere. Thus the cool foggy summer conditions that typify the coastlands of northern California and other similar upwelling regions might, under global warming, become even more pronounced. Effects of enhanced upwelling on the marine ecosystem are uncertain but potentially dramatic.

THE COASTAL OCEAN OFF THE WESTern United States is a classic wind-driven coastal upwelling system (*1, 2*). During the warmer seasons of the year, strong northerly and northwesterly winds induce offshore transport of surface waters. Upwelling of cool, nutrient-enriched water from depth (Fig. 1) balances the resulting loss of surface water near the coast and infuses essential plant nutrients to the surface layers of the ocean. Rich phytoplankton growth supports an abundant trophic pyramid, including valuable fishery resources and important seabird and marine mammal populations (*3*). Cooling and stabilization of the onshore air flow by contact with the upwelled surface waters leads to the cool summer climate of the adjacent coastlands (*4*). Similar upwelling systems occur in the other major subtropical eastern ocean boundary regions; examples are the Canary current system off the Iberian Peninsula and northwestern Africa, the Benguela current system off southwestern Africa, and the Peru current system off western South America. Upwelling in all of these regions tends to be highly seasonal in temperate latitudes, where it peaks in the spring-summer, but tends toward year-round continuity in the more tropical portions (*1*).

The vigorous alongshore wind that drives coastal upwelling in these systems is maintained in part by a strong atmospheric pressure gradient between a thermal low-pressure cell that develops over the heated land mass and the higher barometric pressure over the cooler ocean (*5*). Because of the large-scale atmospheric subsidence occurring in the eastern limbs of the subtropical gyres, and also because of the stabilized, dehumidified onshore air flow, the areas of these coastlands inland of the direct influence of coastal stratus and fog are characterized during the upwelling seasons by dry Mediterranean-type (or desert) climates and clear atmospheric conditions (*4*). The clear conditions lead to strong daytime heating by short-wave solar radiation, particularly in interior valleys such as the Central Valley of California, and rapid nighttime, long-wave radiative cooling.

Recent decades have seen a substantial build-up of CO_2 and other greenhouse gases in the earth's atmosphere (*6*). Resulting inhibition of nighttime cooling and enhancement of daytime heating should lead to intensification of the continental thermal lows adjacent to upwelling regions. This intensification would be reflected in increased onshore-offshore atmospheric pressure gradients, intensified alongshore winds, and accelerated coastal upwelling circulations (Fig. 1). As a positive feedback, the cooling of the ocean surface that results might locally intensify the low-altitude barometric highs at the oceanic sides of the onshore-offshore pressure gradients.

No routine observations of actual rate of upwelling are available. Accordingly, a coastal upwelling index based on an estimate

Pacific Fisheries Environmental Group, Southwest Fisheries Center, National Marine Fisheries Service, National Oceanic and Atmospheric Administration, P.O. Box 831, Monterey, CA 93942.

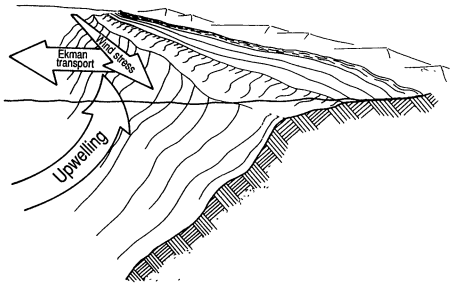

Fig. 1. A conceptual diagram of the coastal upwelling process [modified from (*6*)]. The coast is represented in cutaway view and the ocean is to the left. Offshore transport in the surface Ekman layer driven by the alongshore stress of the wind on the sea surface is replaced by upwelling from depth.

of the alongshore wind stress (that is, the driving force for upwelling) has been used to indicate variations of intensity of upwelling in the California Current region (*5, 7*). Wind observations reported by ships at sea tend to be irregularly distributed in time and space. In order to produce homogeneous time series, the upwelling index computations are based on analyzed fields wherein the geostrophic constraint is employed to incorporate data on both wind and barometric pressure, and information is spread in time and space to fill data voids and to detect erroneous reports (*8*).

The highest intensity core of the California Current upwelling system is situated in the Point Arena–Cape Mendocino region near 39°N (*1*). The equatorward alongshore wind stress during the spring-summer upwelling season, derived on the basis of the upwelling index methodology, has apparently intensified in the 30-year period 1945 to 1975 (Fig. 2A). Since 1975 the stress values have trended back toward the mean for the entire (~40-year) period. Actually, the period since 1975 has been one of anomalously warm conditions in the ocean off California (*9*); whether warm ocean conditions could have affected the onshore-offshore pressure gradient by lessening the relative barometric high at the oceanic end of the gradient is unclear. In any case, substantial, natural interyear and interdecadal variability should be superimposed on any trends related to climatic warming. Certainly, the trend line fitted to the values in Fig. 2A indicates a trend toward substantially increased southward wind stress off the coast of northern California, even over the entire 1946 to 1988 period.

Because of the spatial spreading of information in the analysis procedures, the upwelling index series at different locations in the same region do not represent independent verifications of the trend. However, the index series do reflect significant spatial differences in the California current region (*5, 7*). All of the spring-summer series for this region (Table 1) show a trend toward increased intensity of upwelling-producing wind stress, except for the series located at 24°N and 27°N. These two locations are off Baja California, where the waters of the Gulf of California rather than continental land surface occupy the interior and where therefore the proposed mechanism would be ineffective.

Off the Iberian Peninsula in the northeastern Atlantic Ocean, a 35-year trend toward increased wind stress during the spring to summer upwelling season (Fig. 2B and Table 1) has been reported (*10*). Farther south in the Canary current region (southern Morocco; 28°N), annual mean values of upwelling are available for the period 1946 to 1981 (*11*). In this area, coastal upwelling, while peaking in the summer, tends to persist throughout the year (*12*). Therefore, the use of the mean values, although not ideal, appears acceptable. Again, the general increasing trend is pronounced (Fig. 2C and Table 1).

The upwelling system off Peru presents an extreme tropical case; coastal upwelling continues throughout the year and is actually somewhat more intense in austral winter than in summer (*1*). Because of the low-latitude location and correspondingly weakened geostrophic constraint, upwelling index computations are not appropriate.

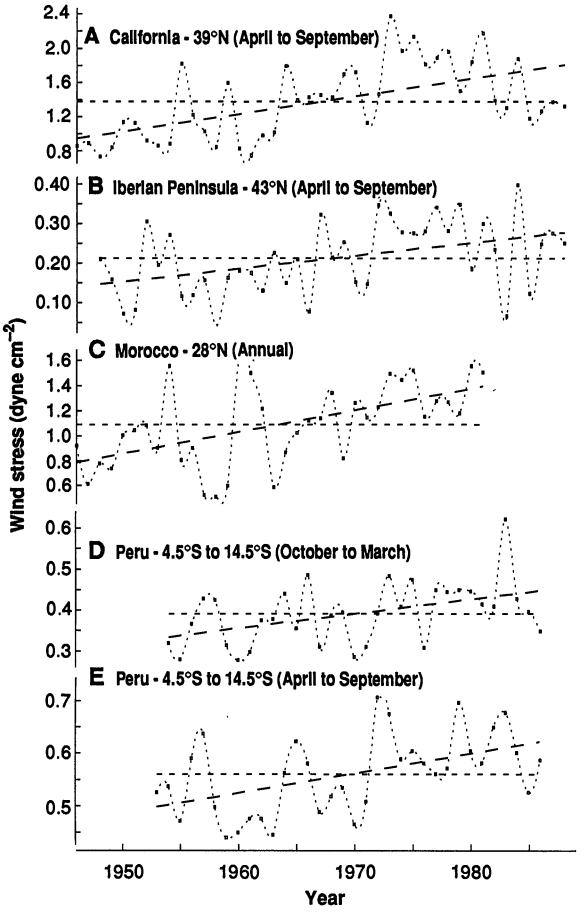

Fig. 2. Within-year averages of monthly estimates of alongshore wind stress off (**A**) California, (**B**) the Iberian Peninsula, (**C**) Morocco, and (**D** and **E**) Peru (in D, each mean value for October to March is assigned to the year in which the January to March portion falls). Short dashes indicate the long-term mean of each series. Longer dashes indicate the linear trend fitted by the method of least squares.

Table 1. Location calendar months incorporated in annual data, slope of the linear trend [significance: * = $P < 0.05$; ** = $P < 0.01$; (*30*)], and standard error of that slope, for averages of monthly alongshore wind stress series.

Latitude or area	Months	Slope (dyne cm^{-2} year^{-1})	Standard error
Upwelling index, northeastern Pacific			
48°N	4 to 9	0.0051**	0.0012
45°N	4 to 9	0.0011	0.0018
42°N	4 to 9	0.0033	0.0032
39°N	4 to 9	0.0206**	0.0044
36°N	4 to 9	0.0102*	0.0046
33°N	4 to 9	0.0136**	0.0050
30°N	4 to 9	0.0022	0.0030
27°N	4 to 9	−0.0041	0.0027
24°N	4 to 9	−0.0021	0.0021
Upwelling index, northeastern Atlantic			
43°N	4 to 9	0.0033**	0.0011
37°N	4 to 9	0.0051**	0.0018
28°N	1 to 12	0.0174**	0.0044
Ship reports, northeastern Atlantic (Fig. 4)			
Area A	4 to 9	0.0101**	0.0024
Area B	4 to 9	0.0048*	0.0022
Area C	4 to 9	0.0060**	0.0018
Area D	4 to 9	0.0064**	0.0016
Ship reports, southeastern Pacific			
Peru	4 to 9	0.0038**	0.0011
Peru	10 to 3	0.0035**	0.0012

Here, wind stress estimates based on individual wind reports from ships at sea have been averaged by month over an area of coastal ocean between 4.5°S and 14.5°S latitudes (*13, 14*). The long-term increasing trend in equatorward alongshore wind stress is not only clearly evident during the spring to summer half of the year (Fig. 2D), but also during fall to winter (Fig. 2E).

The procedures used to derive the various time series from the available data bases have been consistently applied over the entire record. The analyzed data fields forming the data base for the upwelling index computations (*5*) have been routinely produced throughout the record period in support of weather forecasting activities. Because of the extended period of assembly of these data, one wonders if artificial inhomogeneities could have crept in to produce the indicated trend (such as the transition from subjective hand analysis to objective computer analysis, altered data distributions due to changes in shipping routes, or establishment of new coastal reporting stations in data-poor areas). Because the analysis procedures act to spread available information in time and space, one cannot look to upwelling index series computed at nearby locations for independent corroborations.

The area off Spain and Portugal is much higher in maritime data density than the other major eastern ocean upwelling regions, including California (*1*). Here, four strictly independent (sharing no data) series of monthly means of wind stress estimates have been constructed from ship reports available in each of four adjacent 5° latitude by 5° longitude quadrangles (Fig. 3). Although details of the shorter scale interyear variability appear somewhat different among the four series, they all corroborate (Fig. 4 and Table 1) the increasing trend indicated in Fig. 2B.

Thus data from widely separated areas around the world suggest that the equatorward alongshore wind stress that drives coastal upwelling has been increasing during the respective upwelling seasons of the past 40 years. In seasons when upwelling is weak or absent, no consistent pattern of increasing equatorward stress is apparent (for example, off California the slopes of the trend lines for the series of October to March means are weakly negative; off the Iberian Peninsula the fall-winter series exhibit a mixture of weakly positive and weakly negative trends). Thus the increasing trend in equatorward stress is observed only during the upwelling seasons. These are the only seasons during which thermal lows in surface atmospheric pressure develop over the adjacent land mass and therefore in which the hypothesized greenhouse mechanism could operate.

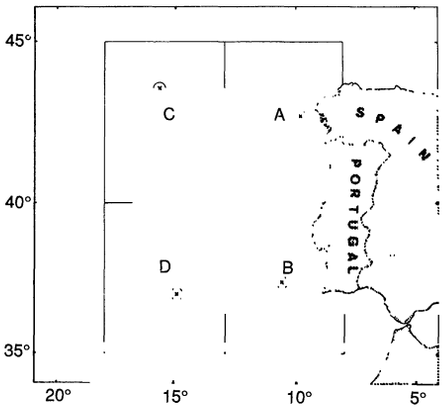

Fig. 3. Four 5° by 5° quadrangles (areas labeled A, B, C, and D) off the Iberian Peninsula in which sea surface wind stress estimates based on maritime wind reports were summarized to produce monthly time series shown in Fig. 4. The mean latitude and longitude of the reports available in each of the areas over the period 1948 to 1979 is marked by an "x" surrounded by a small circle.

When the various series are differenced, effectively removing the linear trends, significant interregional correlation among the time series vanishes. Evidently, the only feature shared among regions is the long-term trend. Other known types of global teleconnections, such as El Niño–Southern Oscillation, are known to be evident in shorter period components of interannual variability. The substantial shorter period interannual variability evident in the time series (Fig. 2) is apparently not shared among regions to any significant degree. A greenhouse mechanism is consistent with the simple monotonically increasing trend that corresponds to the observed interregional pattern. Moreover, simulations of increased atmospheric CO_2 with general circulation models suggest that southward wind stress will increase in the spring and summer off northern California (*15*).

Intensification of coastal upwelling along subtropical and tropical eastern ocean boundaries would have important consequences. Evidently, with increased global warming, the coastal surface waters in these regions could cool relative to the surfaces of either the continental land mass on one side or the ocean interior on the other. With greater temperature contrast at the land-sea boundary, summer sea breezes would tend to be enhanced. Cool, foggy, summer conditions at the coast could become even more pronounced and wind flow through passes in coastal mountain ranges toward the heated interior valleys could strengthen. The onshore air flow might become even more stable and less humid because of enhanced heat loss to the relatively cool ocean surface; thus the coastal zone inland of the fog zone might become even more arid during upwelling seasons.

Effects on the marine ecosystem are more difficult to gauge. Short-term climatic warmings, associated with intense El Niño episodes, have recently occurred in the Peru (*14*) and California (*20*) systems. But the specific dynamics underlying El Niño (*17*) are most likely not identical to those controlling effects of climate warming. Moreover the distribution of biological populations, as well as their abundance, appear often to be more related to the dynamic physical processes that control various patterns in the ecosystem (*18, 19*) than to direct effects of temperature itself. For example, recent empirical results (*20*) indicate that reproductive success of pelagic fishes in upwelling regions depends on the winds being neither so weak that there is insufficient upwelling to enrich the trophic pyramid nor so strong that turbulent mixing of the water column prevents maintenance of fine-scale concentrations of minute food organisms essential to larval survival.

In projecting direct physiological effects of climatic warming on organisms, a first inclination might be to merely increment present characteristic isotherm patterns and to predict changes in biological distributions according to the resulting translocation of

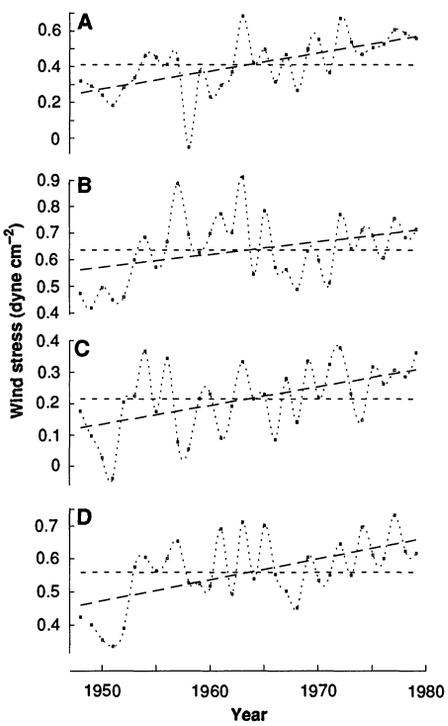

Fig. 4. Six-month (April to September) averages of monthly estimates of alongshore wind stress produced from ship reports within the four areas (A, B, C, and D) shown in Fig. 3. Short dashes indicate the long-term mean of the series. Longer dashes indicate the linear trend fitted by the method of least squares.

temperature ranges. Clearly, there are problems with such a procedure. Also, care must be taken in using evidence from past warm epochs, where various causal aspects of the warming have been somewhat different, to predict the effects of greenhouse warming on the ocean ecosystem. The dynamic ocean processes that determine the temperature distributions could be fundamentally altered.

In the absence of counteracting effects (*21*), intensified upwelling would tend to enhance primary organic production in these systems. But whether this increased primary production would be channeled to trophic components that society particularly values is unclear. There has been little clear demonstration that increased primary production actually promotes reproductive success and population growth of commercial fishes (*19, 22*). For example, increased production might be channeled to the mesopelagic fish communities that are diffused over wide areas and thereby largely lost from the neritic ecosystem. In addition, increased organic production might cause large areas of these systems to become anoxic at depth (*23*) and thereby promote sedimentation of unoxidized organic matter on the sea floor. In any case, if primary production increases, the rate at which carbon is sequestered beneath the ocean thermocline should likewise increase, and thus the rate of buildup of CO_2 in the atmosphere should be reduced.

If greenhouse warming leads to less global temperature contrast between tropical and polar regions, ocean basin–scale atmospheric and ocean circulations might slow down (*24*). However, as this example indicates, there is a competing tendency toward intensification where oceanic-continental temperature contrasts are involved. Many of the consequences of global climate change to marine ecosystems and also to marine-influenced terrestrial systems could depend on the relative importance, in each local situation, of these competing effects.

REFERENCES AND NOTES

1. R. H. Parrish, A. Bakun, D. M. Husby, C. S. Nelson, in (*2*), pp. 731–777.
2. G. D. Sharp and J. Csirke, Eds., *Proceedings of the Expert Consultation to Examine Changes in Abundance and Species Composition of Neritic Fish Resources* (*Fish. Rep. 291*, Food and Agriculture Organization of the United Nations, Rome, 1983).
3. J. H. Ryther, *Science* **166**, 72 (1969); D. Cushing, *Fish. Tech. Pap. 84* (Food and Agriculture Organization of the United Nations, Rome, 1969).
4. G. T. Trewartha, *An Introduction to Climate* (McGraw-Hill, New York, 1968).
5. A. Bakun, *NOAA Tech. Rep. NMFS SSRF671* (1973).
6. V. Ramanathan, *Science* **240**, 293 (1988).
7. J. E. Mason and A. Bakun, *NOAA Tech. Memo. NMFS-SWFC67* (1986).
8. M. M. Holl and B. R. Mendenhall, *Fleet Numeric. Weather Cent. Tech. Note 72-2* (FNOC, Monterey, CA, 1972).
9. D. A. Cole and D. R. McLain, *NOAA Tech. Memo. NMFS-SWFC125* (1989).
10. W. S. Wooster, in preparation; R. R. Dickson, P. M. Kelly, J. M. Colebrook, W. S. Wooster, D. H. Cushing, *J. Plankton Res.* **10**, 151 (1986).
11. H. Belvèze and K. Erzini, in (*2*).
12. W. S. Wooster, A. Bakun, D. R. McLain, *J. Mar. Res.* **34**, 131 (1976).
13. A. Bakun, in *The Peruvian Anchoveta and Its Upwelling Ecosystem: Three Decades of Change*, D. Pauly and I. Tsukayama, Eds. (International Center for Living Aquatic Resources Management, Manila, Philippines, 1987), pp. 46–74; A. Bakun and R. Mendelssohn, in (*14*).
14. D. Pauly, P. Muck, J. Mendo, I. Tsukayama, Eds., *The Peruvian Upwelling Ecosystem: Dynamics and Interactions* (International Center for Living Aquatic Resources Management, Manila, Philippines, in press).
15. M. Torn, in preparation.
16. W. Wooster, D. Fluharty, Eds., *El Niño North* (University of Washington Sea Grant Program, Seattle, 1985).
17. J. Picaut, *Calif. Coop. Oceanic Fish. Inves. Rep.* **26**, 41 (1985).
18. L. Legendre and S. Demers, *Can. J. Fish. Aquat. Sci.* **41**, 2 (1984).
19. A. Bakun, in *L'Homme et les Ecosystems Halieutiques*, J. P. Troadec, Ed. (Institut Français de Recherche pour l'Exploitation de la Mer, Paris, 1990), pp. 155–187.
20. P. Cury and C. Roy, *Can. J. Fish. Aquat. Sci.* **46**, 670 (1989).
21. F. P. Chavez, R. T. Barber, M. P. Sanderson, in (*14*).
22. R. Lasker, in *Toward a Theory of Biological-Physical Interaction in the World Ocean*, B. J. Rothschild, Ed. (Kluwer, Dordrecht, 1989), pp. 173–182.
23. G. A. Jackson *et al.*, *Eos* **70**, 146 (1989); M. S. Quimby-Hunt, P. Wilde, W. N. E. Berry, paper presented at the First Workshop on Global Climate Change and Its Effects on California, University of California, Davis, 10 to 12 July, 1989.
24. On the other hand, the trade winds in the tropical Pacific likewise seem to have increased during this same period [K. D. B. Whysall, N. S. Cooper, G. R. Bigg, *Nature* **327**, 216 (1987)]. Whether seasonally increased alongshore winds along the continental boundaries (equatorward along the eastern ocean boundary, poleward along the western boundary) resulting from enhanced onshore-offshore temperature contrasts could contribute to an increased trade wind circulation is a matter for further study.
25. Indicated significance levels are taken directly from standard tables of the Student's *t* distribution, without adjustment for residual autocorrelation.

11 August 1989; accepted 13 November 1989

Ozone Control and Methanol Fuel Use

A. G. RUSSELL,* D. ST. PIERRE, J. B. MILFORD

Methanol fuel use in motor vehicles and stationary combustion has the potential to improve air quality. A modeling study of methanol fuel use in Los Angeles, California, shows that the low chemical reactivity of methanol vapor slows ozone formation and would lead to lower ozone concentrations. Predicted peak ozone levels decreased up to 16 percent, and exposure to levels above the federal standard dropped by up to 22 percent, when pure (M100) methanol fuel use was simulated for the year 2000. Similar results were obtained for 2010. Use of a gasoline-methanol blend (M85) resulted in smaller reductions. Predicted formaldehyde levels and exposure were not increased severely, and in some cases declined, in the simulations of methanol use.

OVER HALF OF THE PEOPLE IN THE United States live in areas that experience ozone levels above the limits set by the National Ambient Air Quality Standards (NAAQS). Compliance with the standard is proving to be a difficult task. One measure that has been proffered as a solution is the use of alternative, "clean" fuels in motor vehicles. Federal, state, and local agencies are promoting, and have suggested mandating, use of clean fuels in order to reduce ozone and other components of urban smog (*1*). In particular, the use of alternative fuels is integral in the recent plan adopted for the Los Angeles, California, area, and the President's recent proposals would extend the use to other areas. Of the fuels considered, methanol appears to be one of the most feasible for widespread use and improving air quality (*2, 3*). Several studies have shown that methanol, because of its low atmospheric chemical reactivity, could be effective in reducing the formation of photochemical smog and ozone (*3, 4*). The extent of improvement, and whether significant improvement would be realized at all during multiday smog episodes, has been brought into question by recent experiments (*5*). Because methanol-fueled vehicles (MFVs) emit more formaldehyde than their gasoline-fueled counterparts, however, concern has also arisen over the possibility of increased ambient levels of formaldehyde. To evaluate better these concerns and to establish a scientific basis for future strategies, we have used a three-dimensional, Eulerian, photochemical air quality model to investigate how the use of methanol fuel would affect air quality. In this report, we use the model results to address (i) the impact of methanol on atmospheric chemi-

A. G. Russell, Department of Mechanical Engineering, Carnegie Mellon University, Pittsburgh, PA 15213.
D. St. Pierre, Lowry Air Force Base, Denver, CO 80230.
J. B. Milford, Department of Civil Engineering, University of Connecticut, Storrs, CT 06269.

*To whom correspondence should be addressed.